Simvastatin augments activation of liver regeneration through attenuating transforming growth factor-β1 induced-apoptosis in obstructive jaundice rats

DAZHENG FANG[1*], YING HE[2*] and ZHOU LUAN[3]

[1]Department of Hepatobiliary Surgery, Dongfeng General Hospital, Hubei University of Medicine, Shiyan, Hubei 442008;
[2]Department of Ophthalmology, The Central Hospital of Wuhan, Tongji Medical College, Huazhong University
of Science and Technology, Wuhan, Hubei 430014; [3]Department of Gastroenterology, Tongji Hospital, Tongji
Medical College, Huazhong University of Science and Technology, Wuhan, Hubei 430030, P.R. China

Abstract. Obstructive jaundice, owing to biliary obstruction, has been illustrated to trigger various biochemical, histological and immunological changes, leading to liver damage or even failure. The detailed molecular mechanism of simvastatin (Sim) involvement in liver regeneration during obstructive jaundice progression remains poorly elucidated. In the present study, an acute obstructive jaundice rat model was established by ligation and division of common bile duct, which was used to investigate the effects of Sim as a hepatoprotective treatment. Male Sprague-Dawley rats were randomly divided into four groups: Sham-operated, bile duct ligation (BDL) plus saline treatment [0.02 mg/kg/d, intraperitoneally (i.p.)], BDL plus low-dose Sim treatment (0.02 mg/kg, i.p.) and BDL plus high-dose Sim treatment (0.2 mg/kg, i.p.). During this experiment, the BDL+normal saline (NS) group demonstrated increased levels of transforming growth factor-β1 (TGF-β1) expression. Furthermore, Sim-treated animals demonstrated significantly downregulated TGF-β1 expression and improved liver function vs. the BDL+NS group, indicating a TGF-β1 antagonizing function. Additionally, Sim increased hepatocyte DNA synthesis in BDL rats compared to both the BDL+NS and Sham group. Apoptosis was increased in BDL+NS compared to the Sham group, and Sim markedly reduced hepatocyte apoptosis in the BDL group. Moreover, analysis of TGF-β1 signaling pathways demonstrated that there was an increased hepatic TGF-β1 and Smad3 expression in the BDL group, which was attenuated in the presence of Sim. In contrast to TGF-β1, Sim induced the activity of the Smad7 (an inhibitor of TGF-β1 signaling) mRNA and Smad7 protein expression. Sim displays hepatoprotective effects in liver cells via the upregulation of Smad7 expression and impaired TGF-β signaling. Furthermore, the observations of the present study may provide evidence on the mechanism behind Sim blunting TGF-β1 signaling, which is used to ameliorate the complication of liver damage and reduce the mortality rates associated with obstructive jaundice.

Introduction

Obstructive jaundice is a frequently observed symptom in patients undergoing surgery and its major clinical manifestation is a syndrome group, including tissue damage and a series of pathophysiological changes in various systems of the body. These include endotoxemia, infection, liver damage, coagulopathy and malnutrition (1-3). Liver damage caused by obstructive jaundice is an important cause of other complications (4). However, drove of end-stage severe liver injuries by obstructive jaundice still lacks effective therapies (5).

Simvastatin (Sim) is one of the most commonly prescribed drugs for the treatment of hypercholesterolemia since it prevents the synthesis of cholesterol (6). In addition to its lipid-lowering effects, Sim can also protect against cholestasis-induced liver injury (7). However, the molecular mechanisms underlying the hepatoprotective effects of Sim administration on obstructive jaundice remain unknown. The hypothesis considered in the present study was that underlying molecular mechanisms of hepatoprotective Sim effects relate to transforming growth factor-β1 (TGF-β1) signaling during obstructive jaundice progression. Similarly, there is currently a lack of knowledge regarding the effects of TGF-β1 in the early stages of liver damage by obstructive jaundice. TGF-β1 performs a suppressor role in hepatocytes, where it regulates growth and differentiation and induces apoptosis (8). Moreover, the Smads are signal transducers of TGF-β1 (9). Once the ligand binds to the cell surface receptors, Smads are phosphorylated; they

Correspondence to: Dr Zhou Luan, Department of Gastroenterology, Tongji Hospital, Tongji Medical College, Huazhong University of Science and Technology, 1095 Jiefang Road, Wuhan, Hubei 430030, P.R. China
E-mail: luanzhoutj@163.com

*Contributed equally

associate with Smad4, translocate into the nucleus and regulate target gene expression (10). Furthermore, Smad signaling is limited by inhibitory Smad7 (11). Exogenous bone morphogenetic protein 7 (BMP-7) counteracted the effect of TGF-β1 and hepatic fibrosis was ameliorated by the administration of BMP-7 (12).

In the present study, the process of severe liver injury was induced in a rat model by creating obstructive jaundice by double bile duct ligation (BDL). Moreover, the effects of Sim in this rat model were investigated. These observations indicate that the addition of Sim improved liver regeneration and abrogated hepatocyte apoptosis by downregulating the hepatic TGF-β1 signaling pathway in an experimental model of acute obstructive jaundice in rats. However, the specific mechanism underlying this effect remains unclear and requires further investigation.

Materials and methods

Experimental animals and groups. A total of 32 healthy male Sprague-Dawley rats (age, 6-8 weeks; weight, 250-300 g) were provided by the Experimental Animal Center of Tongji Medical College (Wuhan, China). All the rats were housed under habitual conditions at 21 ± 2°C, under a 12-h light/dark cycle and with free access to food and standard laboratory chow. At all times the animals were bred in accordance with the Principles and Guidelines for the Care and Use of Laboratory Animals of Tongji Medical College, recommended by the National Academy of Sciences and published by the National Institute of Health (NIH publication 85-23 revised 1996). The methodology was approved by the Ethics Committee of Tongji Medical College.

The rats were randomly divided into four groups (n=8 per group): i) Sham group, Sham-operated; ii) BDL+NS group, animals underwent BDL and were treated with normal saline (NS; 0.02 mg/kg/day); iii) BDL+Sim 0.02; and iv) BDL+Sim 0.2 groups underwent BDL and were treated with 0.02 or 0.2 mg/kg/day Sim (Sigma-Aldrich; Merck Millipore, Darmstadt, Germany), respectively.

Surgical procedure and sample preparation. Prior to surgery the animals were anesthetized using cotton soaked with 1.5 ml sulfuric ether (Guidechem, Hangzhou, China). Under sterile conditions, an upper abdominal midline incision was performed. Muscle and peritoneal structure were then dissected to expose the common bile duct, which was carefully isolated and double-ligated with a 5-0 silk close to the liver hilus immediately below the bifurcation and cut between the ligatures (BDL group). The control animals underwent a Sham operation in which the common bile duct was not ligated but exposed, and the abdominal incision was then closed using single sutures (13).

In all of the groups the route of administration was intraperitoneal via a single daily injection at 9:00 am for seven days. This route was selected because it appeared to lead to more stable levels of the drug in equilibrium. In total, 24 h after the last injection each animal was weighed, anesthetized with sulfuric ether and sacrificed by exsanguination (abdominal aorta puncture). Blood and tissues were then collected and processed as described below.

Hepatic function parameters. Blood samples were collected with 10 IU/ml sodium heparin (GL Biochem, Shanghai, China) as an anticoagulant, and were then centrifuged at 2,000 x *g* for 5 min at 4°C to obtain plasma. The plasma was then used to measure the total bilirubin (TB), alanine aminotransferase (ALT) and aspartate aminotransferase (AST) as parameters that indicate hepatic function. These biochemical analyses were then performed using an autoanalyzer (7600-020; Hitachi Ltd., Tokyo, Japan).

Western blot analysis. Liver specimens were homogenized in lysis buffer (P0013; Beyotime Institute of Biotechnology, Haimen, China), and the total protein concentration was determined and equalized. The 20 μg samples were then boiled in Laemmli buffer (P0015A; Beyotime Institute of Biotechnology) and analyzed by western blotting as previously described (14). Equal amounts of proteins were separated by 12% SDS-PAGE (P0012A; Beyotime Institute of Biotechnology) with 100 V for 1 h and transferred onto polyvinylidene difluoride membranes (Merck Millipore). The membranes were blocked with 5% bovine serum albumin (Gibco; Thermo Fisher Scientific, Waltham, MA, USA) for 2 h and then incubated with primary antibodies at 4°C overnight. Primary antibodies were used at a dilution of 1:800 and horseradish peroxidase-conjugated secondary antibodies goat anti-mouse IgG (sc-2005) and goat anti-rabblit IgG (sc-2004; both Santa Cruz Biotechnology, Inc., Dallas, TX, USA) at a dilution of 1:5,000. Moreover, detection was performed using Supersignal West Pico chemiluminescent substrate kit (Pierce Protein Biology; Thermo Fisher Scientific, Inc., Rockford, IL, USA) and X-ray film, and was converted to digital images. Densitometric quantification was performed using the Quantity One version 4.62 software (Bio-Rad Laboratories, Inc., Hercules, CA, USA). In all instances, the membranes were stripped and reported using an antibody specific against α-tubulin, and densitometric values were corrected to α-tubulin expression. Furthermore, the commercial antibodies used were: TGF-β1 (ab92486) from Abcam (Cambridge, MA, USA), Smad2 (12584) and Smad3 (9523) from Cell Signaling Technology, Inc. (Danvers, MA, USA) and α-tubulin (sc-8035) from Santa Cruz Biotechnology (Santa Cruz Biotechnology, Inc.).

Immunohistochemistry. Liver tissues were fixed in 10% formalin overnight and embedded in paraffin (327204; Sigma Aldrich, Merck Millipore). Immunohistochemical analysis of the liver tissue was performed as described previously (15), and TGF-β1 expression was detected. Polylysine was smeared on the slides, 3.5-μm paraffin sections were cut and a pressure cooker (WQC50A1P; Midea, Foshan, China) was used to prepare the hot citric acid antigen for primary TGF-β1 antibody repair (sc-130348; 1:100; Santa Cruz Biotechnology, Inc.). It was then incubated for 1 h with a biotin-conjugated secondary antibody, goat anti-mouse IgG-B (sc-2039; 1:800; Santa Cruz Biotechnology, Inc.), at room temperature for 30 min, 3,3'-diaminobenzidine (DAB) colored for 5-10 min and stained with hematoxylin and eosin for 1-3 min. An Olympus Corporation (Tokyo, Japan) BX51 microscope was used to photograph the slides. Phosphate-buffered saline (PBS) instead of the primary antibody was used as a negative

control. Using a Leica Qwin V3 image analysis system (Leica Microsystems GmbH, Wetzlar, Germany), immunohistochemical analysis of the positive products of the area in each section was selected at a magnification of x200 of the three non-overlapping representations. The percentage of each sample was then calculated and the positive area (positive area/measurement area) was determined. The scoring criteria used based on a semiquantitative approach, in which the percentage of TGF-β1-positive cells (0-100%) was determined and multiplied by the staining intensity (0, negative; 1, weak; 2, moderate; 3, strong).

Total RNA extraction and reverse transcription-quantitative polymerase chain reaction (RT-qPCR). Total RNA from liver was extracted using TRIzol (Invitrogen; Thermo Fisher Scientific, Inc.) reagent according to the manufacturer's instructions and treated with RNase-free DNaseI (Invitrogen; Thermo Fisher Scientific, Inc.) following the manufacturer's protocol. In total, 2 μg total RNA from liver was reverse transcribed into cDNA using the StrataScript first-strand synthesis system (Stratagene; Agilent Technologies, Inc., Santa Clara, CA, USA). TGF-β1 (sense: 5'-AGGGCTTTC GCTTCAGTGCT-3' and anti-sense: 5'-CCATGAGGAGCA GGAAGGGT-3'); Smad3 (sense: 5'-TGAACACCAAGTGCA TTACCA-3' and anti-sense: 5'-TGACTGGCTGTAGGTCCA AGT-3'), and Smad7 (sense: 5'-CGGAATTCGCCACCA TGTTCAGGACCAAACGATC-3' and anti-sense: 5'-CGG GATCCACTACCGGCTGTTGAAGATG-3') were amplified using SYBR Green PCR master mix (Applied Biosystems; Thermo Fisher Scientific, Inc.) and iCycler real-time PCR detection system (Bio-Rad Laboratories, Inc.) for 40 cycles. Relative levels were then calculated using the iCycler software and a standard equation (Applied Biosystems; Thermo Fisher Scientific, Inc.) and normalized against glyceraldehyde 3-phosphate dehydrogenase (sense: 5'-CCTGGTATGACA ATGAATATG-3' and anti-sense: 5'-TCTCTTGCTCTCAGT ATCC-3').

Terminal deoxynucleotidyl transferase-mediated deoxyuridine triphosphate nick-end labeling (TUNEL) assay. Hepatocyte apoptosis was quantified using the TUNEL assay. All liver tissue specimens were fixed in freshly prepared 3.5% paraformaldehyde (158127; Sigma-Aldrich; Merck Millipore) and sucrose (V900116 Sigma-Aldrich; Merck Millipore). Tissues were then embedded in Thermo Shandon Cryomatrix (Thermo Fisher Scientific, Inc.), sectioned (10 μm) using a Shandon Cryotome (M16512), and then stored at 4˚C. After treating the specimen with PBS, the sections were processed following the instructions of an *In Situ* Cell Death Detection Kit (Roche Diagnostics, Indianapolis, IN, USA). After rinsing the specimens twice with PBS, the tissue peroxidase activity was visualized using DAB. TUNEL-positive nuclei were counted in five high-powered fields and expressed as a percentage of the total nuclei counted (16). Moreover, two investigators (one of which was blinded) scored the sections, and the mean of the two scores is reported.

Proliferating cell nuclear antigen (PCNA) labeling index. PCNA immunostaining was performed in order to examine the hepatocyte proliferation with the mouse monoclonal antibody against PCNA (clone-PC 10; 1:100; Dako Denmark A/S, Glostrup, Denmark). Briefly, remnant liver tissue specimens were fixed in 10% buffered formalin, embedded in paraffin and then cut into 5-μm sections. The deparaffinized sections were then treated by microwave heating thrice in PBS for 5 min each, then washed three times with PBS for 5 min each. Following blocking with endogenous peroxidase, the specimens were washed three times with PBS for 5 min each. The sections were then incubated with the antibody against PCNA overnight at 4˚C. After washing several times with PBS, biotin-labeled secondary antibody (sc-57636; 1:2,000; Santa Cruz Biotechnology) was added for 1 h at room temperature, and after washing several times with PBS the tissue peroxidase activity was visualized using DAB (17). The PCNA labeling index was then determined as the number of PCNA-positive cells among 1,000 counted cells at high power (magnification, x400).

Statistical analysis. Statistical comparison was performed using GraphPad Prism version 5.0 (GraphPad Software, Inc., San Diego, CA, USA). Student's *t*-test, Welch's *t*-test or Mann-Whitney U test were adapted for the evaluation of the significance of the differences between groups. P<0.05 was used to indicate a statistically significant difference. Results are expressed as the mean ± standard error.

Results

General condition. The urine color of the rats evidently deepened 24 h-post operation. After 48 h, the tails of these rats began to turn yellow. Following prolonged bile duct obstruction, there was progression in jaundice, and the appetite and mental states gradually deteriorated.

Effect of Sim on hepatic architecture and function. Sections from hepatic tissue from the four experimental groups were analyzed after hematoxylin and eosin staining (Fig 1), however, no histopathological differences were observed between the control group (Fig. 1A) and animals receiving Sim (Fig. 1D). By contrast, BDL caused substantial hepatocellular injury, as indicated by a >7.2-fold increase in liver enzymes. However, Sim treatment significantly reduced BDL-induced liver damage (Fig. 1B and C; P<0.01 vs. BDL+NS group). Moreover, the BDL+NS group significantly elevated the serum TB by >17.6-fold vs. the Sham group, suggesting that an obstructive jaundice model was successfully established (Fig. 1E). Bilirubin levels in rats treated with Sim following BDL were not different from those in NS-treated animals, indicating that the degree of obstructive jaundice was similar in all of the experimental groups (Fig. 1E). Moreover, administration of 0.02 mg/kg/day Sim significantly suppressed the release of ALT and AST from the liver by 61.02 and 58.01%, respectively, compared with the NS-treated rats. The treatment with 0.2 mg/kg/day Sim decreased BDL-induced ALT and AST levels by 69.14 and 65.18%, respectively (Fig. 1F and G; P<0.01 vs. BDL+NS group).

Inhibition of the TGF-β1 signaling pathway by the addition of Sim. TGF-β1 concentrations in the liver were significantly elevated in the livers of BDL animals compared with those

in Sham-operated animals (P<0.01) (Fig. 2A, B and E). Sim administration markedly lowered obstructive jaundice-induced elevation of hepatic concentration of TGF-β1 (P<0.01) (Fig. 2E). Moreover, RT-qPCR and western blot analyses revealed that TGF-β1 was less activated in the liver tissues obtained from Sim-treated rats compared to those from NS-treated rats (Fig. 2F and G). These results indicate that Sim administration blunted the TGF-β1 signaling pathway that is known to contribute to the aggression of obstructive jaundice-induced liver injury.

TUNEL assay. TUNEL immunohistochemistry stained liver sections taken from Sham, BDL+NS, BDL+ Sim 0.02 and BDL+ Sim 0.2 are shown in Fig. 3A-D. Immunohistochemistry for TUNEL demonstrated a significant increase in TUNEL-positive hepatocytes after BDL compared to the Sham group (P<0.01) (Fig. 3A and B). Furthermore, treatment of BDL animals with Sim resulted in a significant reduction in the percentage of hepatocyte apoptosis compared to BDL rats treated with saline (P<0.01) (Fig. 3B and D). Also, in the Sham animals no significant change on apoptosis was noted (Fig. 3A).

PCNA assay. PCNA immunohistochemistry stained liver sections were collected following seven days of BDL. Sham, BDL+NS, BDL+Sim 0.02 and BDL+Sim 0.2 are depicted in Fig. 4A-D. Immunohistochemical staining for PCNA demonstrated a significant increase in DNA synthesis in the BDL+NS group, compared to the Sham group (Fig. 4B). Moreover, treatment of BDL rats with Sim increased DNA synthesis in BDL animals to 27% compared to the controls (Fig. 4C and D).

Discussion

Obstructive jaundice has been identified as a significant risk for patients resulting from surgery, which may result in alterations of the glycogen metabolism, decreased cell-mediated immunity, impaired hepatic and renal functions, increased circulating endotoxins and a depressed synthesis of homeostasis factors (18). These factors can decrease the tolerance of patients to anesthesia and surgery, leading to an increasing operative risk (19).

In the present study, the addition of Sim was demonstrated to improve liver regeneration and abrogated hepatocyte apoptosis by downregulating the hepatic TGF-β1 signaling pathway in an experimental model of acute obstructive jaundice in rats. These observations demonstrate that acute obstructive jaundice by ligation and division of the common bile duct induces liver damage. Furthermore, the addition of Sim significantly enhances liver regeneration and alleviates hepatic dysfunction by downregulating the hepatic TGF-β1 signaling pathway in an experimental model of acute obstructive jaundice in rats. The hepatic Sim content decreases after liver injury (4), and it is likely that Sim administration facilitates liver regeneration. Moreover, Sim inhibits collagen processing leading to increased ubiquitination and decreased secretion in hepatic stellate cells (HSCs) (20). Additionally, Sim prevents liver injury induced by alcohol in rats by reducing liver lipid peroxidation, anti-inflammation and antihyperplasia (21). Conversely,
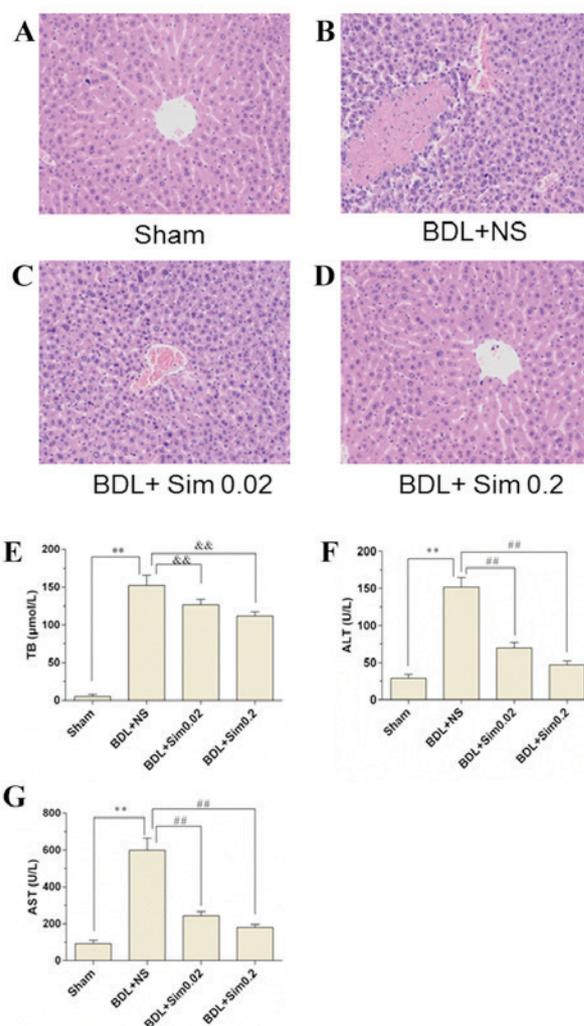
Figure 1. Effect of Sim on the hepatic architecture and function. Hematoxylin and eosin staining of sections from hepatic tissue from (A) Sham, (B) BDL+NS, (C) BDL+ Sim 0.02 and (D) BDL+Sim 0.2 groups (magnification, x400). The levels of (E) TB, (F) ALT and (G) AST were determined. Data are expressed as the mean ± standard error of the mean. **P<0.01 vs. Sham group; &&P>0.05 and ##P<0.01 vs. BDL+NS group. TB, total bilirubin; BDL, bile duct ligation; NS, normal saline; ALT, alanine aminotransferase; AST, aspartate aminotransferase.

during liver regeneration by partial hepatectomy, inhibition of the liver regeneration by Sim may be mediated by liver fat accumulation (22). Finally, prevention from the decrease in the intracellular content of Sim, as a factor attenuating regeneration remains unclear.

The presently investigated hypothesis was that the underlying molecular mechanisms of hepatoprotective Sim effects relate to TGF-β1 signaling during obstructive jaundice progression. Obstructive jaundice alters serum TGF-β1 expression in the rat and oral bile acid or glutamine (or both) can restore the altered serum TGF-β1 expression in rats that have obstructive jaundice (23). In addition, an important protective mechanism of Sim against fibrosis may be to lower TGF-β levels and the activation of collagen I production, and particularly to repress the activation of the collagen type I alpha 2 chain (COL1A2) gene by preventing TGF-β effects on its responsive site in the COL1A2 promoter (24).
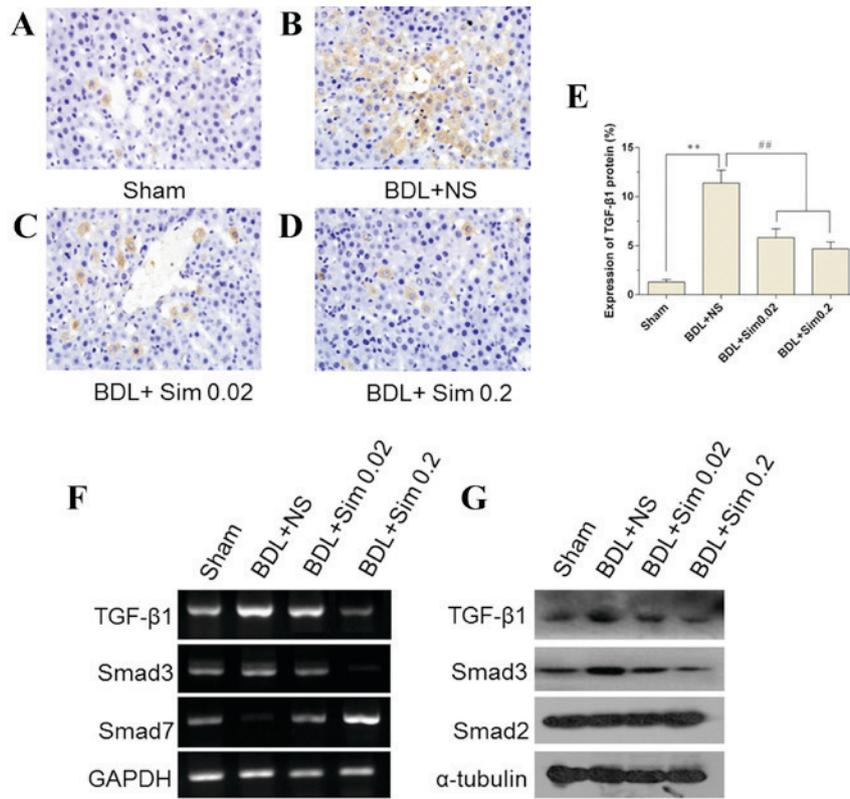
Figure 2. Sim blunts the hepatic TGF-β1 signaling pathway in the liver of obstructive jaundice rats. Representative immunohistochemical images of TGF-β1 from (A) Sham, (B) BDL+NS, (C) BDL+ Sim 0.02 and (D) BDL+Sim 0.2 groups (magnification, x400). (E) The levels of TGF-β1 from the images shown above were determined. (F) Reverse transcription-polymerase chain reaction analysis demonstrated that the TGF-β1 signaling pathway was less activated in the livers obtained from Sim-treated rats than those obtained from NS-treated rats. (G) Western blot analysis demonstrated the results of the western blot above. Data are expressed as the mean ± standard error of the mean. **P<0.01 vs. Sham group; ##P<0.01 vs. BDL+NS group. BDL, bile duct ligation; NS, normal saline; TGF-β1, transforming growth factor-β1; GAPDH, glyceraldehyde 3-phosphate dehydrogenase.
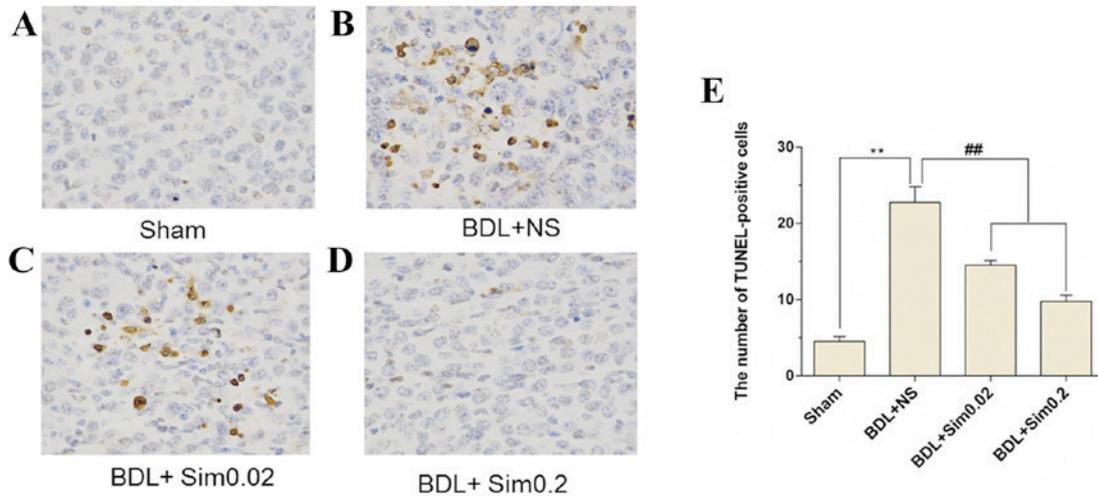
Figure 3. TUNEL immunohistochemistry-stained liver sections taken from (A) Sham, (B) BDL+NS, (C) BDL+ Sim 0.02 and (D) BDL+Sim 0.2 groups (magnification, x400). (E) The number of TUNEL-positive cells from the images shown above was determined. Data are expressed as the mean ± standard error of the mean. **P<0.01 vs. Sham group; ##P<0.01 vs. BDL+NS group. BDL, bile duct ligation; NS, normal saline; TUNEL, terminal deoxynucleotidyl transferase dUTP nick end labeling.

In the present study Sim appeared antagonize TGF-β1 in hepatic cells though the induction of Smad7 expression. Moreover, anti-TGF-β1 action may target collagen expression. TGF-β1 is secreted by transdifferential hepatic cells, and quiescent hepatic cells are highly responsive to exogenous TGF-β1 (25). Smad3, an intracellular mediator of TGF-β1 signal transduction, binds to the TbRE and stimulates COL1A2 transcription when overexpressed in HSCs, but
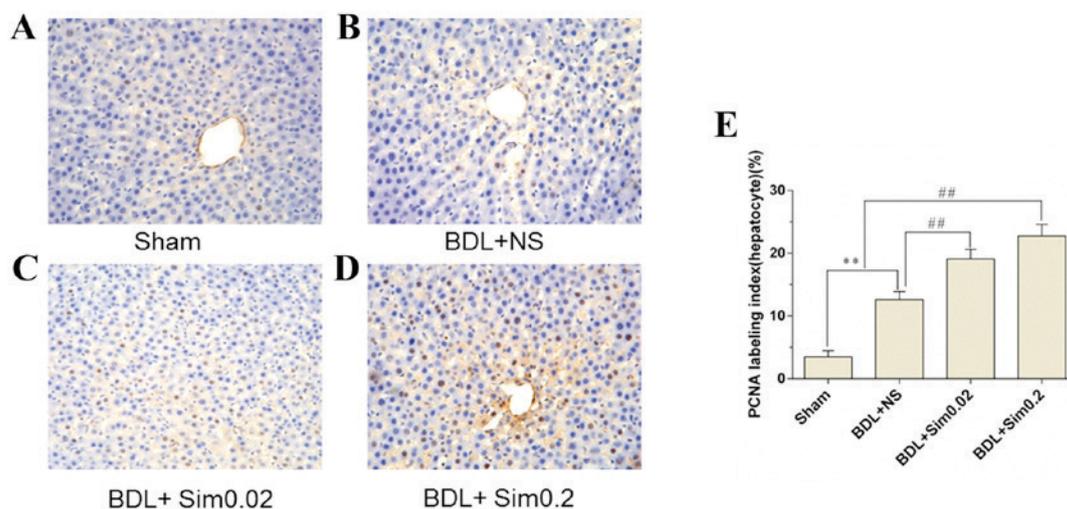
Figure 4. Immunohistochemical staining for PCNA from (A) Sham, (B) BDL+NS, (C) BDL+S Sim 0.02 and (D) BDL+S Sim 0.2 groups (magnification, x400). (E) PCNA labeling index from above images was determined. Data are expressed as mean ± standard error of the mean. **P<0.01 vs. Sham group; $^{##}$P<0.01 vs. BDL+NS group. BDL, bile duct ligation; NS, normal saline; PCNA, proliferating cell nuclear antigen.

increased COL1A2 gene transcription of the cells is not affected by overexpression of inhibitory Smad7 (26). In addition, TGF-β downregulates the alcohol metabolizing enzyme alcohol dehydrogenase 1 mRNA in cultured hepatocytes and liver tissue from TGF-β transgenic mice via the ALK5/Smad2/3 signaling branch, with Smad7 as a potent negative regulator (27). Conversely, TGF-β1 represses the gene transcription of 7α-hydroxylase in human hepatocytes by a mechanism involving Smad3-dependent inhibition of HNF4α and HDAC remodeling of 7α-hydroxylase chromatin (28).

The inhibition of epidermal growth factor receptor in hepatocellular carcinoma enhanced TGF-β-induced pro-apoptotic signaling (29). TGF-β-induced apoptosis in rat hepatocytes does not have the need for Rac-dependent nicotinamide adenine dinucleotide phosphate oxidases, and TGF-β upregulates the Rac-independent Nox4, which is associated with its pro-apoptotic activity (30). Moreover, caffeine downregulates TGF-β-induced connective tissue growth factor (CTGF), CTGF expression in hepatocytes by the stimulation of degradation of the TGF-β effector Smad2, inhibition of Smad3 phosphorylation and upregulation of the peroxisome proliferator-activated receptor γ (31).

The present study on the rat BDL model similarly points to anti-TGF-β1 effects of Sim. These are Sim-reduced intrinsic and TGF-β1 gene activity and phosphorylation of Smad2/3 proteins. The latter is due to the following mechanism: i) Sim-dependent decline in the expression level of Smad2/3 was observed in parallel with the downregulation of phosphorylation; and ii) Smad7 expression was initiated by Sim. Among the acute phase of liver injury, expression of the Smad7 protein is rapidly increased by TGF-β1 signaling and fibrotic signals mediated by Smad are inhibited (32). However, a lack of Smad7 expression as a prerequisite for disease progression is further suggested by the observation that tissue fibrosis in rats is inhibited by ectopic Smad7 expression (33).

In conclusion, the data of the present study provide evidence on the mechanism of how Sim blunts profibrotic TGF-β1 signaling. There is a causal association between Sim administration and the TGF-β1 signaling pathway following BDL. Moreover, the addition of Sim abrogates the harmful hepatocyte apoptosis and beneficially augments hepatic regeneration during obstructive jaundice progression. In addition, this mechanism may provide the clues to improved ways that will ameliorate the complication of liver damage and reduce the morbidity and mortality of obstructive jaundice.

Acknowledgements

References

1. Kimmings AN, van Deventer SJH, Obertop H, Rauws EA, Huibregtse K and Gouma DJ: Endotoxin, cytokines, and endotoxin binding proteins in obstructive jaundice and after preoperative biliary drainage. Gut 46: 725-731, 2000.
2. Addley J and Mitchell RM: Advances in the investigation of obstructive jaundice. Curr Gastroenterol Rep 14: 511-519, 2012.
3. Fang Y, Gurusamy KS, Wang Q, Davidson BR, Lin H, Xie X and Wang C: Meta-analysis of randomized clinical trials on safety and efficacy of biliary drainage before surgery for obstructive jaundice. Br J Surg 100, 1589-1596, 2013.
4. Okaya T, Nakagawa K, Kimura F, Shimizu H, Yoshidome H, Ohtsuka M, Morita Y and Miyazaki M: Obstructive jaundice impedes hepatic microcirculation in mice. Hepatogastroenterology 55: 2146-2150, 2008.
5. Yeki M, Koda M, Matono T, Sugihara T, Maeda K and Murawaki Y: Preventative and therapeutic effects of perindopril on hepatic fibrosis induced by bile duct ligation in rats. Mol Med Report 2: 857-864, 2009.
6. Jadhav SB and Jain GK: Statins and osteoporosis: New role for old drugs. J Pharm Pharmacol 58: 3-18, 2006.
7. Dold S, Laschke MW, Lavasani S, Menger MD, Jeppsson B and Thorlacius H: Simvastatin protects against cholestasis-induced liver injury. Br J Pharmacol 156: 466-474, 2009.
8. Hayashi H, Sakai K, Baba H and Sakai T: Thrombospondin-1 is a novel negative regulator of liver regeneration after partial hepatectomy through transforming growth factor-beta1 activation in mice. Hepatology 55: 1562-1573, 2012.

9. Ren M, Wand B, Zhang J, Liu P, Lv Y, Liu G, Jiang H and Liu F: Smad2 and Smad3 as mediators of the response of adventitial fibroblasts induced by transforming growth factor β1. Mol Med Report 4: 561-567, 2011.
10. Hill CS: Nucleocytoplasmic shuttling of Smad proteins. Cell Res 19: 36-46: 2009.
11. Derynck R and Zhang YE: Smad-dependent and Smad-independent pathways in TGF-β family signaling. Nature 425: 577-584, 2003.
12. Yang T, Chen SL, Lu XJ, Shen CY, Liu Y and Chen YP: Bone morphogenetic protein 7 suppresses the progression of hepatic fibrosis and regulates the expression of gremlin and transforming growth factor β1. Mol Med Rep 6: 246-252, 2012.
13. Tao YY, Wang QL, Shen L, Fu WW and Liu CH: Salvianolic acid B inhibits hepatic stellate cell activation through transforming growth factor beta-1 signal transduction pathway in vivo and in vitro. Exp Biol Med (Maywood) 238: 1284-1296, 2013.
14. Luan Z, He Y, Alattar M, Chen Z and He F: Targeting the prohibitin scaffold-CRAF kinase interaction in RAS-ERK-driven pancreatic ductal adenocarcinoma. Mol Cancer 13: 38, 2014.
15. Wu MH, Cao W, Ye D, Ren GX, Wu YN and Guo W: Contactin 1 (CNTN1) expression associates with regional lymph node metastasis and is a novel predictor of prognosis in patients with oral squamous cell carcinoma. Mol Med Rep 6: 265-270, 2012.
16. Canbay A, Hiquchi H, Bronk SF, Taniai M, Sebo TJ and Gores GJ: Fas enhances fibrogenesis in the bile duct ligated mouse: A link between apoptosis and fibrosis. Gastroenterology 123: 1323-1330, 2002.
17. Bird MA, Black D, Lange PA, Samson CM, Hayden M and Behrns KE: NFkappaB inhibition decreases hepatocyte proliferation but does not alter apoptosis in obstructive jaundice. J Surg Res 114: 110-117, 2003.
18. Tsuyuguchi T, Takada T, Miyazaki M, Miyakawa S, Tsukada K, Nagino M, Kondo S, Furuse J, Saito H, Suyama M, et al: Stenting and interventional radiology for obstructive jaundice in patients with unresectable biliary tract carcinomas. J Hepatobiliary Pancreat Surg 15: 69-73, 2008.
19. Lacaine F, Fourtanier G, Fingerhut A and Hay JM: Surgical mortality and morbidity in malignant obstructive jaundice: A prospective multivariate analysis. Eur J Surg 161: 729-734, 1995.
20. Rombouts K, Kisanga E, Hellemans K, Wielant A, Schuppan D and Geerts A: Effect of HMG-CoA reductase inhibitors on proliferation and protein synthesis by rat hepatic stellate cells. J Hepatol 38: 564-572, 2003.
21. Wang W, Zhao C, Zhou J, Zhen Z, Wang Y and Shen C: Simvastatin ameliorates liver fibrosis via mediating nitric oxide synthase in rats with non-alcoholic steatohepatitis-related liver fibrosis. PLoS One 8: e76538, 2013.
22. Slotta JE, Laschke MW, Schilling MK, Menger MD, Jeppsson B and Thorlacius H: Simvastatin attenuates hepatic sensitization to lipopolysaccharide after partial hepatectomy. J Surg Res 162: 184-192, 2010.
23. Sheen-Chen SM, Eng HL and Hung KS: Altered serum transforming growth factor-beta1 and monocyte chemoattractant protein-1 levels in obstructive jaundice. World J Surg 28: 967-970, 2004.
24. Itoh Y, Kimoto K, Imaizumi M and Nakatsuka K: Inhibition of RhoA/Rho-kinase pathway suppresses the expression of type I collagen induced by TGF-beta2 in human retinal pigment epithelial cells. Exp Eye Res 84: 464-472, 2007.
25. Lv Z and Xu L: Salvianolic acid B inhibits ERK and p38 MAPK signaling in TGF-β1-stimulated human hepatic stellate cell line (LX-2) via distinct pathways. Evid Based Complement Alternat Med 2012: 960128, 2012.
26. Zhang W, Ou J, Inagaki Y, Greenwel P and Ramirez F: Synergistic cooperation between Sp1 and Smad3/Smad4 mediates transforming growth factor beta1 stimulation of alpha 2(I)-collagen (COL1A2) transcription. J Biol Chem 275: 39237-39245, 2000.
27. Ciuclan L, Ehnert S, Ilkavets I, Weng HL, Gaitantzi H, Tsukamoto H, Ueberham E, Meindl-Beinker NM, Singer MV, Breitkopf K and Dooley S: TGF-beta enhances alcohol dependent hepatocyte damage via down-regulation of alcohol dehydrogenase I. J Hepatol 52: 407-416, 2010.
28. Li T and Chiang JY: A novel role of transforming growth factor beta1 in transcriptional repression of human cholesterol 7alpha-hydroxylase gene. Gastroenterology 133: 1660-1669, 2007.
29. Caja L, Sancho P, Bertran E and Fabregat I: Dissecting the effect of targeting the epidermal growth factor receptor on TGF-β-induced-apoptosis in human hepatocellular carcinoma cells. J Hepatol 55: 351-358, 2011.
30. Carmona-Cuenca I, Roncero C, Sancho P, Caja L, Fausto N, Fernandez M and Fabregat I: Upregulation of the NADPH oxidase NOX4 by TGF-beta in hepatocytes is required for its pro-apoptotic activity. J Hepatol 49: 965-976, 2008.
31. Gressner OA, Lahme B, Rehbein K, Siluschek M, Weiskirchen R and Gressner AM: Pharmacological application of caffeine inhibits TGF-beta-stimulated connective tissue growth factor expression in hepatocytes via PPARgamma and SMAD2/3-dependent pathways. J Hepatol 49: 758-767, 2008.
32. Tahashi Y, Matsuzaki K, Date M, Yoshida K, Furukawa F, Sugano Y, Matsusshita M, Himeno Y, Inagaki Y and Inoue K: Differential regulation of TGF-beta signal in hepatic stellate cells between acute and chronic rat liver injury. Hepatology 35: 49-61, 2002.
33. Dooley S, Hamzavi J, Breitkopf K, Wiercinska E, Said HM, Lorenzen J, Ten Dijke P and Gressner AM: Smad7 prevents activation of hepatic stellate cells and liver fibrosis in rats. Gastroenterology 125: 178-191, 2003.